# Mobile Robots with Novel Environmental Sensors for Inspection of Disaster Sites with Low Visibility

Project start: January 1, 2015

Duration: 3.5 years

# Deliverable 2.8

# Gas Source Localization

Due date: month 40 (April 2018)

Lead beneficiary: ORU

## Dissemination Level: Public

## Main Authors:

Victor Hernandez Bennetts (ORU)

Erik Schaffernicht (ORU)

Han Fan (ORU)


## Version History:

0.2: First revision, VH, ES, HF. May, 2018

0.1: initial version, VH, April, 2018

## Contents

Contents ... 3
A Introduction and purpose of this document ... 4
B Indicators for Gas Source Proximity ... 4
C Experimental Runs ... 5
D Summary and Outlook ... 8
References ... 9

# A Introduction and purpose of this document

The task of Gas Source Localization (GSL) is essential for applications that require the detection and monitoring of volatile chemicals. GSL is one of the key questions addressed by Mobile Robot Olfaction (MRO), the research area that enables gas sensing for mobile robots. A common approach for GSL is to assume that gases disperse in a pre-defined way (e.g. Gaussian-like plumes) and that a laminar wind flow exists. Thus, it is possible to follow concentration gradients towards the gas source. Such approach to GSL is commonly referred to as plume tracking [1]. In Smokebot, gradient-based and plume tracking approaches are not applicable. In a post-disaster scenario, rubble, highly uneven temperature gradients and turbulence-dominated airflow prevent the formation of smooth, Gaussian-like gas distributions (Fig. 1.A and 1.B). In addition, plume tracking algorithms make the implicit assumption that only one gas source is present and no interferents (such as smoke) exists. In a disaster scenario, this assumption does not hold. Moreover, the Smokebot platform is expected to conduct different tasks during an exploration mission and thus, the platform cannot plan its trajectory solely focused on GSL exploration.

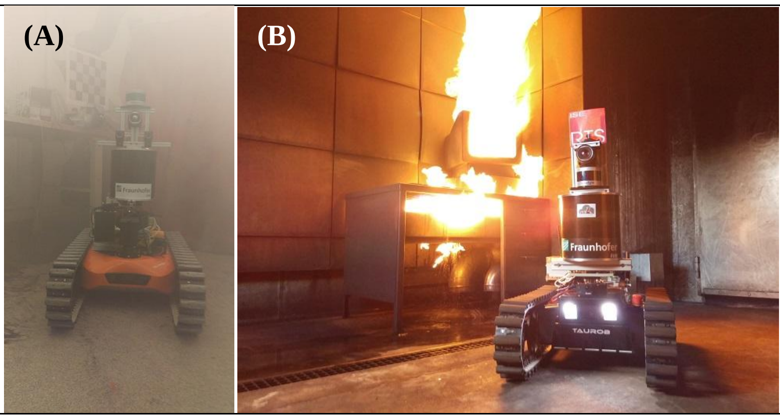


**Fig. 1:** Two examples of scenarios where the Smokebot platform is expected to operate. (A) Smoke-saturated locations. (B) A location with uneven temperature distributions due to fire hazards.

Thus, D2.8 moves away from plume tracking in favor of statistically-oriented approaches [2] that leverage on features (i.e. indicators) such as the time variability of the sensor response. Such statistically-oriented approaches can provide operators with a set of hypotheses (or suggestions) of locations likely to contain gas sources. These hypotheses can be identified as the robot explores the environment and conducts other tasks. This is in stark contrast to the plume tracking case where the robot is solely focused on following cues towards a gas source. To evaluate the applicability of the approach, we use two commonly used source proximity indicators, namely the average concentration level and the fluctuations (i.e. variance) of the gas concentration [3]. In addition, we propose a probabilistic indicator based on the predictions of an improved version of the unsupervised gas discrimination algorithm presented in D2.6. Thus, the proposed source proximity estimator uses the learned gas discrimination model in order to predict probability of the presence of gas at different locations. A key advantage of the proposed indicator is that it provides estimations between defined upper and lower boundaries (0 and 1). This is an advantage over mean and variance-based indicators which do not have an upper boundary and thus require the definition thresholds in order to filter out small changes in the sensors' responses. Moreover, when using arrays of multiple sensors like on the Smokebot platform, a sensor selection process is required in order to identify the most accurate sensor.

# B Indicators for Gas Source Proximity

Several authors have studied the use of the distribution of gas concentrations in the environments as a way to localize gas sources [4]. For example, locations that exhibit a high value on the mean gas concentration readings can be a good indicator of the presence of a gas source under certain environmental conditions. However, it has also been shown that the location of the highest average gas concentration does not always correlate with the location of a gas source [5] for example, when gas accumulates at a particular location (like in a corner away from the source). In addition, it has also been that statistical moments can be used as indicators of gas source proximity [3]. More specifically, it has been demonstrated that the fluctuations (i.e. variance) of the sensor response can be used to estimate the source proximity since high sensor response variance is observed closer to a gas source. Another indicator that is highly correlated to the variance in the sensor response was proposed by Schmuker and co-authors in [6], where events of rapid change in the MOX sensor signal ("bouts") are identified and counted in order to estimate the distance to a gas source.

In Smokebot, we proposed a novel proximity indicator which uses a learning algorithm to determine the probability of the presence of gas ($\mathbf{p_{gas}}$) given the readings from an array of gas sensors. The proposed estimator $\mathbf{p_{gas}}$ uses an updated version of the unsupervised gas discrimination approach (D2.6), which was recently published in [7]. In this improved version, the discrimination models are learned and updated online as data is being collected. Updates on the discrimination model depend on gas detection events observed during robot exploration. Such events are modeled through the state machine shown in Fig. 2.

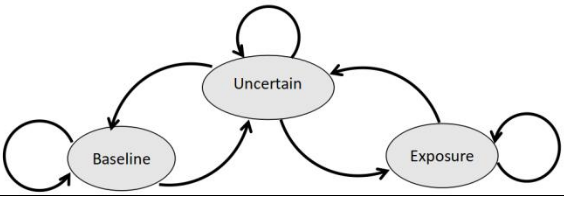


**Fig. 2:** State machine used to model the presence/absence of gas exposure events.

As shown in Fig. 2, the state machine has three states, namely baseline state, uncertain state and exposure state. The baseline state corresponds to clean air exposure. Measurements collected in this state are used to learn an adaptive model of the baseline. This process is used to diminish the effects of baseline drift, which is a hardware limitation of, e.g., MOX sensors. The uncertain state corresponds to measurements recognized to be different from baseline, but deemed not informative enough to trigger an update on the gas classification model. The exposure state represents events at which analytes are detected. When the state machine transitions to the exposure state, a re-learning process is triggered and carried out using measurements collected during the exposure state. At the core of this online, unsupervised gas discrimination approach is the KmP algorithm (D2.6), which consists of three phases namely the K-phase, the m-phase and the P-phase. The K phase learns the number of chemical compounds, while the m phase learnes the detection threshold of the e-nose and finally, the P phase assigns class posteriors to the acquired measurements. Once baseline and discrimination models have been updated, the system can be queried in order to determine $\mathbf{p_{gas}}$ given the current measurement.

## C Experimental Runs

In order to evaluate the different proximity indicators, we conducted experiments in Örebro University main campus. The experimental scenario is a basement with a narrow corridor connecting two rooms, where two gas sources of different type were placed at separated locations (Fig. 3.A). The Smokebot platform was equipped with two different MOX sensor arrays, namely a commercial array (ORU nose) and a prototype array composed of high bandwidth sensors (UWAR nose) developed by UWAR as part of deliverables D2.4 and D2.5 (Fig. 3.B). A total of seven experiments were conducted using this experimental setup.

In the experimental runs, two gas sources of different kind were placed in the environment. The gas sources were generated using a container filled with ethanol, propanol or acetone (Fig. 3.A). To facilitate evaporation, a bubbler was used. The robot never moved closer than 0.5m to the gas sources. Before the start of the experiment, the sensor arrays were allowed to pre-heat for a period of time between 10 and 30 minutes. In addition, a few minutes were spent away from the gas sources to learn the baseline level (i.e. the sensor response to clean air). The robot was then remote controlled to explore the target location in order to collect measurement at different locations. As the data was being collected, the KmP algorithm was performing adaptive gas discrimination. Table 1 summarizes the experimental conditions.

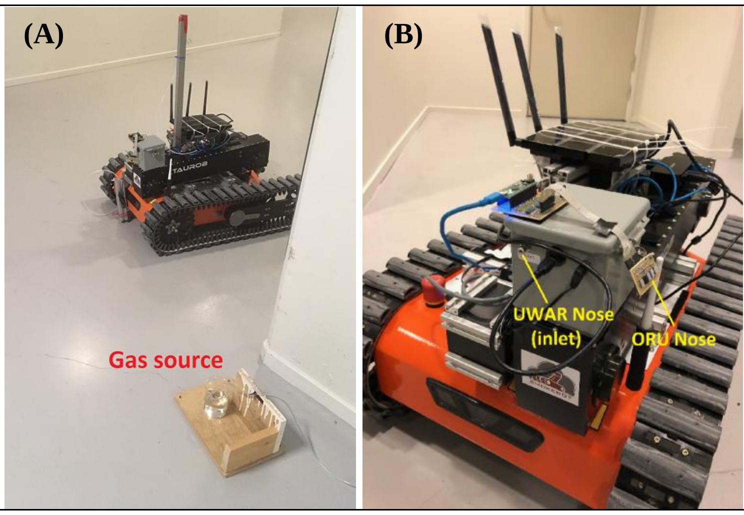


**Fig. 3:** (A) Experimental scenario. (B) Gas sensing payload on-board the Smokebot platform.

Regarding the sensing payload, the high bandwidth array (UWAR nose) incorporates three MOX sensors coated with tin oxide ($SnO_2$), tungsten oxide ($WO_3$) and nickel oxide (NiO), respectively. During the sampling process, the ambient air is drawn into an internal pipe work by a micro air pump. An airflow rate sensor is employed to monitor the volumetric flow rate, which is used as a reference measure to control the pump speed. The measurements are filtered by a physical filter to eliminate the smoke particles, and further moved into a gas measurement chamber to interact with the MOX sensors. The raw sensor responses are generated at 100 Hz, and they are pre-processed by an on-board micro-controller in real-time with digital filters, peak detection and fast Fourier transform (see D2.5 for details). With what respects to the ORU nose, 6 commercial MOX sensors, namely, MICS2614, MICS5524, MICS5914, MICS2714 and a dual MICS4514 were used. Contrary to UWAR nose, the sensors are not housed inside a chamber but instead, they are directly exposed to the environment in what is commonly referred to as an open sampling configuration [8]. The sensors in the ORU nose are fabricated by SGX Sensortech[1] and according to the manufacturer; they are highly sensitive to volatile organic compounds. For both sensor arrays, the sampling frequency was set to 2Hz.

| Nr | Date | Start time | Duration | Source 1 | Source 2 |
|---|---|---|---|---|---|
| 1 | 2018-03-27 | 18:00 | 31 minutes | Ethanol | Acetone |
| 2 | 2018-03-28 | 11:51 | 43 minutes | Ethanol | Acetone |
| 3 | 2018-03-29 | 10:56 | 21 minutes | Ethanol | Propanol |
| 4 | 2018-03-29 | 11:44 | 26 minutes | Ethanol | Propanol |
| 5 | 2018-03-30 | 09:00 | 18 minutes | Ethanol | Propanol |
| 6 | 2018-03-30 | 09:54 | 20 minutes | Ethanol | Propanol |
| 7 | 2018-05-02 | 09:00 | 15 minutes | --- | --- |

**Table 1:** Experiment summary.

[1] https://www.sgxsensortech.com/

To evaluate the proximity indicators, data from the first six experiments were used. The experimental area was divided using a grid with cell size equal to 1m. Mean ($\mu$), variance (v) and the probability of the presence of gas ($\mathbf{p}_{gas}$) were computed for each cell and for each sensor in the e-noses. In addition, $\mu_a$ and $v_a$ were computed for each nose. These indicators correspond to the average over all the sensors in the e-nose. Fig. 4 shows the results for the experiments were propanol and acetone were released in the environment. Notice that in the case of $\mu$, the location of the maximum depends on the selection of the sensor. While sensor 3 is able to localize the gas source 0.5m from the measurement position (which was the actual position of the source), the rest of the sensors (and the averaged indicator $\mu_a$) localize the source at 1.5m. In the case of the variance, the gas source was predicted at 1.5m from the measurement position. For $\mathbf{p}_{gas}$, the source was estimated to be at 0.5m from the measurement location, which corresponds to the actual location of the source. Notice that $\mu_3$ and $\mathbf{p}_{gas}$ are equally accurate. However, to identify $\mu_3$ as the most accurate sensor in the array, a selection process would be required. Such selection process requires the acquisition of training data, a time demanding process.

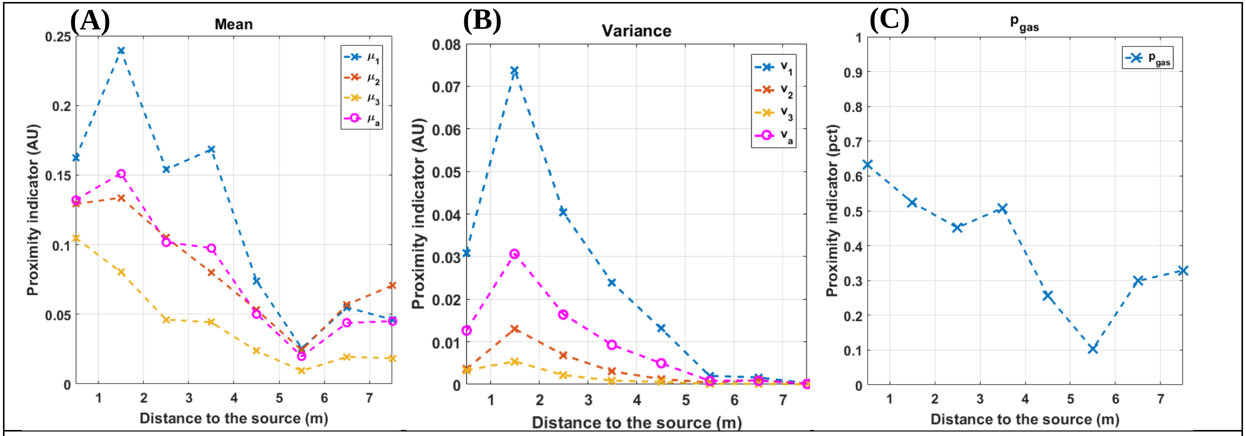


**Fig. 4:** Proximity indicators in the presence of ethanol and acetone. (A) Mean, (B) Variance, (C) $\mathbf{p}_{gas}$

Another advantage of using $\mathbf{p}_{gas}$ as a proximity indicator is shown in Fig. 5. Such plots correspond to experiments conducted with a non-emitting source located at coordinates [0,0]. For the mean-based and variance-based indicators, peaks are located at different locations. While these peaks are smaller, when compared to experiments where emitting gas sources were present (see Fig. 4), a mean/variance threshold needs to be learned in order to filter out small changes in the sensor response. Notice, on the other hand, that the $\mathbf{p}_{gas}$ indicator is rather constant, close to 0%. Hence the absence of an emitting gas source is recognized correctly.

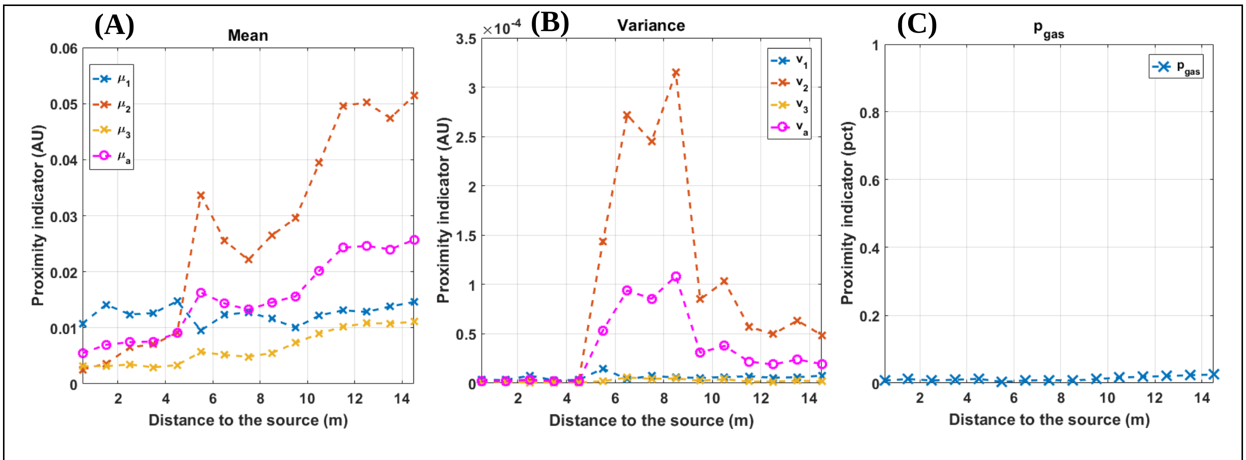


**Fig. 5:** Proximity indicators when no source is present in the environment. (A) Mean, (B) Variance, (C) $\mathbf{p}_{gas}$

Fig. 6.A and Fig. 6.B show error bars of the overall performance for the different indicators for each sensor in the UWAR nose and the ORU nose. Such error bars were computed using data for the six experiments where emitting gas sources were present. The indicator $\mathbf{p_{gas}}$ has a rather consistent performance over the whole experimental dataset. In the case of the ORU nose, $\mathbf{p_{gas}}$ is the second-best indicator overall (predicting the location of the gas source at an average distance of 1m) while for the UWAR nose, $\mathbf{p_{gas}}$ outperforms all the indicators (along with μ3) while predicting the gas source location at an average distance of 0.75m. As previously mentioned, the actual distance to the source was at least 0.5m for all experiments.

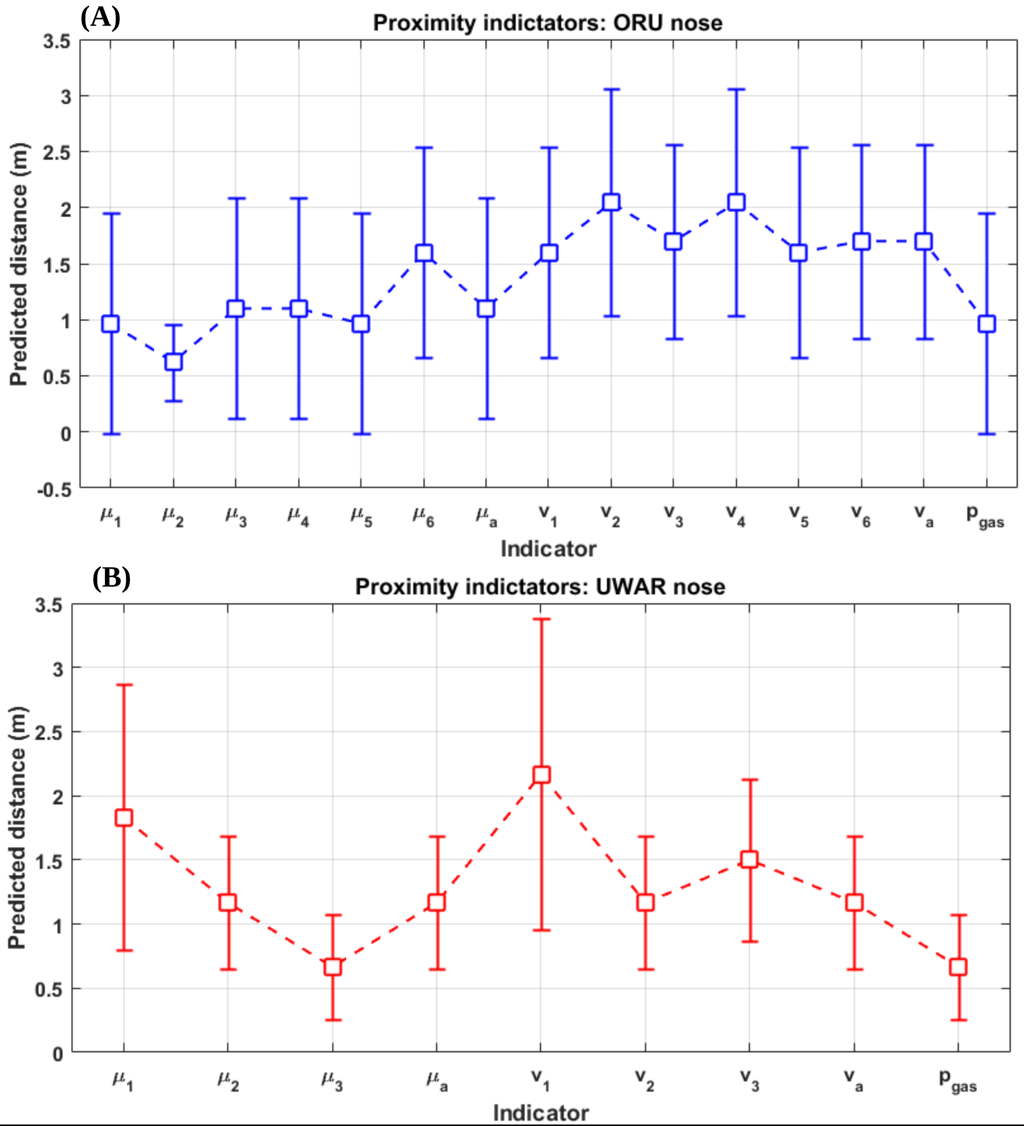


**Fig. 6:** Overall performance for the different sensors and proximity indicators. (A) ORU nose. (B) UWAR nose

## D Summary and Outlook

In the Smokebot application scenario, the presence of gas interferents, obstacle-ridden environments, uneven temperature distributions and turbulent air flows prevents the use of commonly used gas distribution approaches such as plume tracking. Instead, Smokebot focuses on the use of statistically-oriented approaches that provide Smokebot operators with a series of hypotheses about the location of the gas source. Such hypotheses are presented in the form of indicators that reach their maxima when a source is located at near proximity of the measurement location.

In Smokebot we evaluated two commonly used indicators, namely the mean concentration level and the variance of the sensor response and we found that, while both indicators can be rather accurate, there are shortcomings that have to be taken into consideration. First, when using an e-nose, a sensor selection process is needed in order to find the most accurate sensor in the array, which requires the acquisition of training data. This is a considerable challenge in the case of Smokebot, where target compounds and the identity of interferents is unknown. Second, mean-based and variance-based indicators do not have an upper boundary and thus, such indicators do not provide a probabilistic estimation of the gas source presence. Third, thresholds are required to be learned in order to discard readings that correspond to small changes in the sensor response.

Thus we proposed a novel gas source proximity indicator named based on an online, unsupervised gas discrimination algorithm. The proposed indicator, referred to as the probability of the presence of gas ($\mathbf{p}_{\mathbf{gas}}$) does not have the shortcomings of mean-based and variance-based indicators and when evaluated with real-world data, it showed a consistent performance that often outperformed the previously mentioned indicators.

## References


**[1]** G. Kowadlo and A. Russell. Robot Odor Localization: A Taxonomy and Survey The International Journal of Robotics Research. Volume: 27 issue: 8, page(s): 869-894

**[2]** V. Hernandez Bennetts, A. J. Lilienthal, P. P. Neumann and M. Trincavelli. Mobile robots for localizing gas emission sources on landfill sites : is bio-inspiration the way to go?. Frontiers in Neuroengineering, 4(20):1-12, 2012

**[3]** A. J. Lilienthal, H. Ulmer, H. Fröhlich, F. Werner and A. Zell, Learning to Detect Proximity to a Gas Source with a Mobile Robot. Proceedings of the IEEE/RSJ International Conference on Intelligent Robots and Systems (IROS), 2004, pp. 1444-1449.

**[4]** A. J. Lilienthal, T. Duckett, F. Werner, and H. Ishida, "Indicators of Gas Source Proximity using Metal Oxide Sensors in a Turbulent Environment," in Proceedings of the IEEE / RAS-EMBS International Conference on Biomedical Robotics and Biomechatronics (Biorob), February 20 – 22 2006

**[5]** T. Lochmatter, Bio-Inspired and Probabilistic Algorithms for Distributed Odor Source Localization using Mobile Robots. Ph.D. Thesis, EPFL, Lausanne, Switzerland, February 2010

**[6]** M. Schmuker, V. Bahr, and R. Huerta, "Exploiting plume structure to decode gas source distance using metal-oxide gas sensors", Sensor and Actuator B-Chemical, vol. 235, pp. 636-646, 2016

**[7]** H. Fan, V. Hernandez Bennetts, E. Schaffernicht and A. Lilienthal. A cluster analysis approach based on exploiting density peaks for gas discrimination with electronic noses in open environments. Sensors and actuators. B, Chemical, 259:183-203, 2018

**[8]** Marco Trincavelli, Gas Discrimination for Mobile Robots . Künstliche Intelligenz, 25: 4, 2011, pp. 351-354